Pattern formation induced by a differential shear flow

L. Stucchi[1,2] and Desiderio A. Vasquez[2,3]

[1]*Departamento Académico de Ingeniería, Universidad del Pacífico, Apartado 4683, Lima, Perú*

[2]*Departamento de Ciencias, Sección Física, Pontificia Universidad Católica del Perú, Apartado 1761, Lima, Perú*

[3]*Department of Physics, Indiana University–Purdue University Fort Wayne, Fort Wayne, Indiana 46805, USA*

(Received 19 April 2012; revised manuscript received 1 November 2012; published 21 February 2013)

Fluid flow advecting one substance while others are immobilized can generate an instability in a homogeneous steady state of a reaction-diffusion-advection system. This differential-flow instability leads to the formation of steady spatial patterns in a moving reference frame. We study the effects of shear flow on this instability by considering two layers of fluid moving independently from each other, but allowing the substances to diffuse along and across the layers. We find that shear flow can generate instabilities even if the average flow velocity is zero for both substances. These instabilities are strongly dependent on which substance is advected by the shear flow. We explain these effects using the results of Taylor dispersion, where an effective diffusivity is enhanced by shear flow.

DOI: 10.1103/PhysRevE.87.024902 PACS number(s): 89.75.Kd, 47.54.−r, 82.40.Ck

I. INTRODUCTION

Chemical pattern formation can be generated by fluid flow in reaction-diffusion-advection systems which leads to mechanisms such as the differential flow instability (DIFI) [1] or the flow-distributed oscillation (FDO) [2,3]. These instabilities differ from the mechanism predicted by Turing [4], caused exclusively by different diffusivity coefficients. The DIFI mechanism predicts instead that a homogeneous steady state will lose stability when fluid flow advects one substance while the others remain still. Nonuniform shear flow advecting all substances can also generate instabilities [5]. These effects can be reproduced replacing the flow with a simpler two-layer model, which also leads to chemical pattern formation [6]. Experiments already show that a uniform flow advecting one substance can induce a DIFI instability [7,8]. Thus, the effects of shear flow should be relevant to further experiments that rely on fluid flow to generate patterns.

In this Brief Report we explore the effects of shear flow on the DIFI instability, using a standard cubic autocatalator as the reaction term, which has been extensively used to study instabilities with fluid flow [9,10]. We assume that both substances have the same diffusivity, thus eliminating the possibility of Turing pattern formation. We will show that the effects of shear flow strongly depend on which substance is advected. We also show that this mechanism can be modeled using the results of Taylor dispersion.

II. THE MODEL

The DIFI instability takes place in reaction-diffusion-advection systems where different substances are advected by different velocity fields [1]. The spatiotemporal behavior for concentrations of two substances can be described with a system of two equations in dimensionless form:

$$\frac{\partial X}{\partial t} + \vec{V}_X \cdot \vec{\nabla} X = \nabla^2 X + f(X,Y) \tag{1}$$

and

$$\frac{\partial Y}{\partial t} + \vec{V}_Y \cdot \vec{\nabla} Y = \delta \nabla^2 Y + g(X,Y). \tag{2}$$

Here t corresponds to time, the operator $\vec{\nabla}$ corresponds to the gradient, and ∇^2 indicates the Laplacian operator. The functions X and Y represent the dimensionless concentrations of each substance advected by different velocity fields $\vec{V}_X$ and $\vec{V}_Y$. The parameter δ describes the ratio between their diffusivities ($\delta = D_Y/D_X$). In this Brief Report we focus on the case where $\delta = 1$ to avoid interactions with other types of diffusive instabilities. We choose the cubic autocatalator model for the reaction terms [11], thus

$$f(X,Y) = X^2 Y - X \tag{3}$$

and

$$g(X,Y) = \mu - X^2 Y. \tag{4}$$

Here X acts as an activator and Y as an inhibitor, with μ measuring the constant rate of production of Y. The cubic autocatalator has been widely used to study DIFI instabilities [9,12,13], and their interaction with other types of instabilities and patterns, such as the Turing instability and the flow-distributed structures (FDS) [10,14].

In the one-dimensional model with equal diffusivities, the DIFI instability depends only on the relative velocity between substances. This happens regardless of which one is moving relative to the laboratory frame since a simple change to a moving reference frame will set any of the species stationary with the others moving relative to this one [10]. A homogeneous stable steady state then loses stability once the relative velocity reaches a threshold. In the present work we consider the effects of shear flow on the DIFI instability. For shear flow to occur, the velocity field cannot be uniform. Therefore we need to choose a fluid velocity field that will vary in the direction perpendicular to the moving fluid, as is the case of a simple two-layer model. In this two-layer model, fluid flows constantly in each layer with different velocities, thus generating shear flow. In order to notice the difference we will consider the case where only the inhibitor flows with shear flow, and the opposite case, where only the activator flows with shear flow.

Diffusion across the layers acts through a parameter R, which is the same for both species since we are considering the case of equal diffusivities ($\delta = 1$). The concentrations in each layer are represented by the functions X_i, Y_i, where

the subindex i labels the concentration in a particular layer ($i = 1,2$). Therefore the set of reaction-diffusion-advection equations [Eqs. (1) and (2)] becomes a system of four coupled equations. For the case where only the inhibitor is advected the set of equations becomes

$$\frac{\partial X_1}{\partial t} = \frac{\partial^2 X_1}{\partial x^2} + R\,(X_2 - X_1) + f(X_1, Y_1), \tag{5}$$

$$\frac{\partial Y_1}{\partial t} + \left(\bar{V} + \frac{V_r}{2}\right)\frac{\partial Y_1}{\partial x} = \frac{\partial^2 Y_1}{\partial x^2} + R\,(Y_2 - Y_1) + g(X_1, Y_1), \tag{6}$$

$$\frac{\partial X_2}{\partial t} = \frac{\partial^2 X_2}{\partial x^2} + R\,(X_1 - X_2) + f(X_2, Y_2), \tag{7}$$

$$\frac{\partial Y_2}{\partial t} + \left(\bar{V} - \frac{V_r}{2}\right)\frac{\partial Y_2}{\partial x} = \frac{\partial^2 Y_2}{\partial x^2} + R\,(Y_1 - Y_2) + g(X_2, Y_2), \tag{8}$$

where the velocities of Y corresponding to each layer are characterized with an average velocity $\bar{V}$ and a relative velocity between layers V_r. Equations are similar for the case where only the activator is advected, the only difference being that the advection terms apply to X. Having $V_r = 0$ indicates no shear flow, with the DIFI instability caused by a uniform velocity [10].

The reaction-diffusion-advection equations [Eqs. (5)–(8)] allow a homogeneous steady solution with $X_1 = X_2 = X_0 = \mu$ and $Y_1 = Y_2 = Y_0 = \mu^{-1}$. We test the stability of this state to small perturbations of fixed wavelength by replacing $X_i = X_0 + X_i' e^{\lambda t} e^{ikx}$, and $Y_i = Y_0 + Y_i' e^{\lambda t} e^{ikx}$ into Eqs. (5)–(8). Neglecting the nonlinear terms results in a set of coupled linear equations for the amplitudes X_i' and Y_i'. Requiring that the set of equations has a nontrivial solution leads to a polynomial equation on the eigenvalues λ. This leads to a dispersion relation between λ and the wave number k determining the stability of the steady state.

III. RESULTS

A. Linear stability analysis

We analyze the stability of the homogeneous steady state obtaining the growth rate λ as a function of the wave number k. The stability of the system will be determined by the real part of the growth rate ($\mathrm{Re}\,\lambda$). In the case where $\mathrm{Re}\,\lambda < 0$ small perturbations will vanish with time, indicating a stable steady state. We focus on the dependence of $\mathrm{Re}\,\lambda$ on k to determine the stability with respect to perturbations of a fixed wave number. In order to solve the equations numerically, we need to choose values for the diffusive coupling between the layers R and the autocatalator parameter μ. We chose $R = 25$, which is a convenient value to show the effects of shear flow. The steady state for the autocatalator, without diffusion and advection, is unstable for $\mu < 1$. Since we are looking for instabilities caused by advection, we use the value of $\mu = 1.4$, which provides a stable steady state for the reaction alone.

We compare the case where the activator is advected (with no advection for the inhibitor) to the opposite case, where only the inhibitor is advected. Our results are shown in Fig. 1, where we display the real part of the growth rate λ as a function of k, for different V_r. For $k = 0$ the matrix is independent of V_r and diffusion, having a growth rate equal to -0.48, indicating stability for the reaction term alone. For the first case, we set the average velocity of the flow to $\bar{V} = 5$, since for this situation the system presents an instability when $V_r = 0$, as predicted in the one-layer problem [10]. However, after increasing V_r beyond 16.4, the maximum for $\mathrm{Re}\,\lambda$ becomes negative, indicating that the homogeneous steady state becomes stable for all perturbations [Fig. 1(a)]. Consequently, shear flow advecting only the activator acts as a stabilizing mechanism. Figure 1(b) shows that the opposite effect occurs when the shear flow advects only the inhibitor. Here we set the value of the average velocity flow to be $\bar{V} = 0$. Without any fluid flow $V_r = 0$, the system is stable. However, as we increase

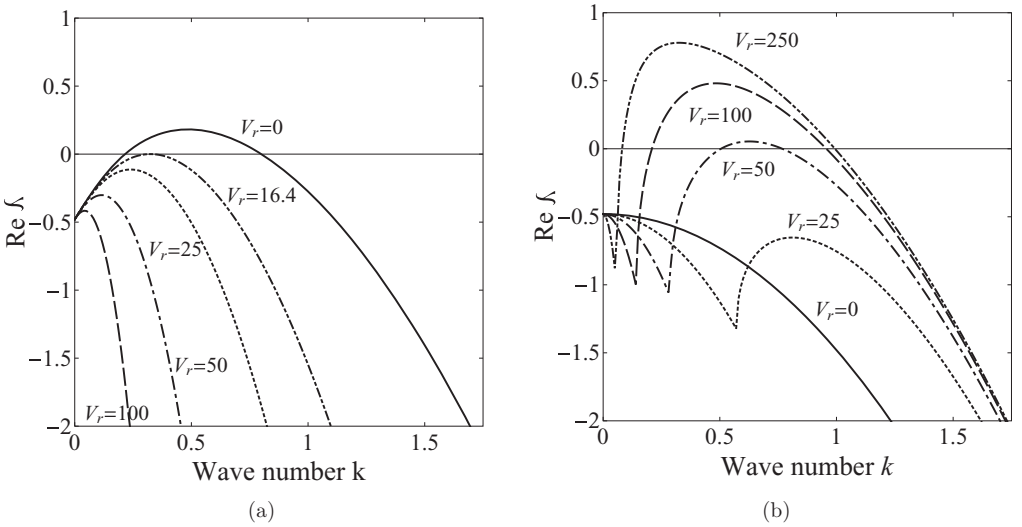

FIG. 1. Real part of the growth rate $\mathrm{Re}\,\lambda$ as a function of wave number k. Each curve corresponds to a different value of V_r. (a) Only the activator is advected. We set the average velocity to $\bar{V} = 5$. When there is no shear flow ($V_r = 0$) the homogeneous steady state is unstable, but if we increase V_r, the instability disappears. (b) Only the inhibitor is advected. The average velocity is set to $\bar{V} = 0$, therefore the instability is due only to shear flow. Here $\mu = 1.4$ and $R = 25$.

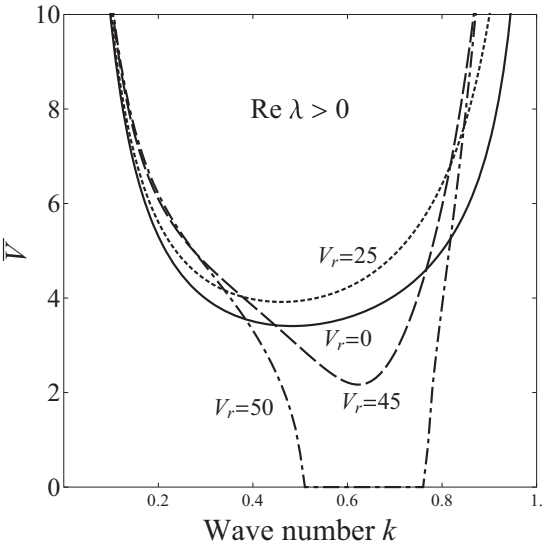

FIG. 2. Neutral stability curves for different values of the velocity between layers V_r. In this case the advected substance is the inhibitor. Minima of the curves $\bar{V}_c$ are the critical average velocities, above these values the system becomes unstable. For small V_r the corresponding values of $\bar{V}_c$ increase, however, for $V_r > 41$ the values of $\bar{V}_c$ decrease. In the case of $V_r = 50$, no net flow is necessary to generate an instability. Here $\mu = 1.4$ and $R = 25$.

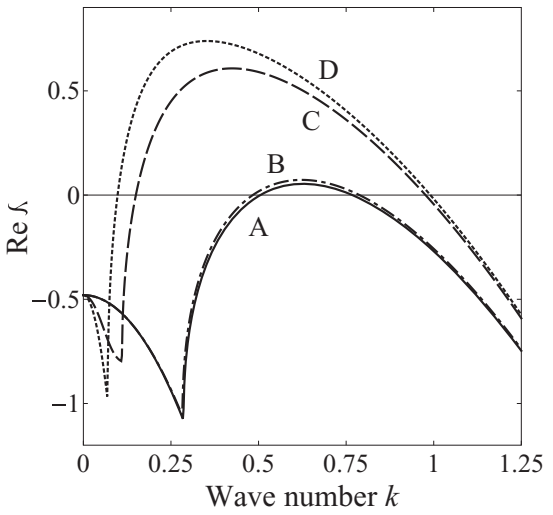

FIG. 3. Comparison of Re $\lambda(k)$ for the linear stability analysis on the two-layer system and using a Taylor dispersion approximation. Here only the inhibitor is advected by a shear flow ($V_r = 50$). For $R = 25$, we have curve (A) corresponding to the two-layer system and curve (B) to the Taylor dispersion approximation. When $R = 1.5$, we have curve (C) for the two-layer system and curve (D) for the Taylor dispersion approximation. This shows that Taylor dispersion is appropriate only when R has higher values. Here $\mu = 1.4$ and $\bar{V} = 0$.

the values of V_r, the system becomes unstable, indicating an instability caused by the shear flow alone for $V_r > 47$. Since this is the type of instability we are interested in, further analysis considers only the case where shear flow advects only the inhibitor.

In Fig. 2 we display the average velocity $\bar{V}$ necessary to make this system unstable given a perturbation of wave number k and a fixed value of V_r. Here we show that the marginal stability curve has a minimum critical velocity $\bar{V}_c$. When $V_r = 0$, our results correspond again to the one-dimensional model [10]. In this case, the corresponding critical average velocity is $\bar{V}_c = 3.41$. An imposed shear flow have two different effects on the stability of the homogeneous steady state. For small values of V_r, the critical velocity $\bar{V}_c$ increases, increasing the region of stability. This behavior continues up to $V_r < 25$. However, for $V_r > 25$, the critical velocity $\bar{V}_c$ begins to decrease, consequently decreasing the region of stability. The value of $\bar{V}_c$ remains higher than without shear flow up to $V_r < 41$. For $V_r > 41$, $\bar{V}_c$ becomes lower than the critical average velocity without shear flow. This results in a system which is more unstable compared to systems with the same average velocity but no shear flow. Finally, when $V_r > 47$, the critical average velocity reaches 0 and no net flow is needed to have an unstable system, a result that was already discussed in Fig. 1(b).

B. Taylor dispersion

We can understand the effects of shear flow on the DIFI instability in terms of Taylor dispersion. This effect corresponds to an enhancement of the diffusivity of a substance advected by shear flow leading to an effective diffusion coefficient [15]. In the original work, Taylor considered a diffusive chemical advected by a Poiseuille flow inside a cylindrical pipe. The substance diffuses with an effective diffusivity along the pipe, once it had enough time to diffuse in the radial direction, roughly a time equal to a^2/D, where a is the radius of the pipe. The enhancement of the diffusion coefficient depends on the type of shear flow advecting the substance. In the case of diffusion in a two-layer flow, the effective diffusivity corresponds to $D_{\text{eff}} = D + V_r^2/8R$ after a time of the order of $1/R$ [16]. According to this result, diffusion in a two-layer flow can be approximated with a flow of uniform velocity $\bar{V}$ and an effective diffusivity that involves the shear effects, namely, the relative velocity between the layers V_r. With these substitutions, the system effectively becomes the one-dimensional single-layer system previously studied in the literature. We carry out the linear stability analysis on this effective system and compare it to the full calculation in Fig. 3. Here we display the dispersion relation between Re λ and the wave number k for different values of the parameter R using two different methods: one with the formula for the effective diffusivity D_{eff}, and the other with the exact calculation for the two layers. In both cases we use the same relative velocity between the layers $V_r = 50$ advecting only the inhibitor. The average front speed $\bar{V}$ is set to zero. The figure shows that using the results of Taylor dispersion provides a good approximation for the linear stability analysis. This approximation is better if the coupling parameter R is relatively large. The results corresponding to $R = 25$ are better approximated by the Taylor dispersion formula than the results for $R = 1.5$, as shown clearly in Fig. 3.

C. Nonlinear numerical results

We solved numerically the nonlinear reaction-diffusion-advection equations [Eqs. (5)–(8)] with parameters in the

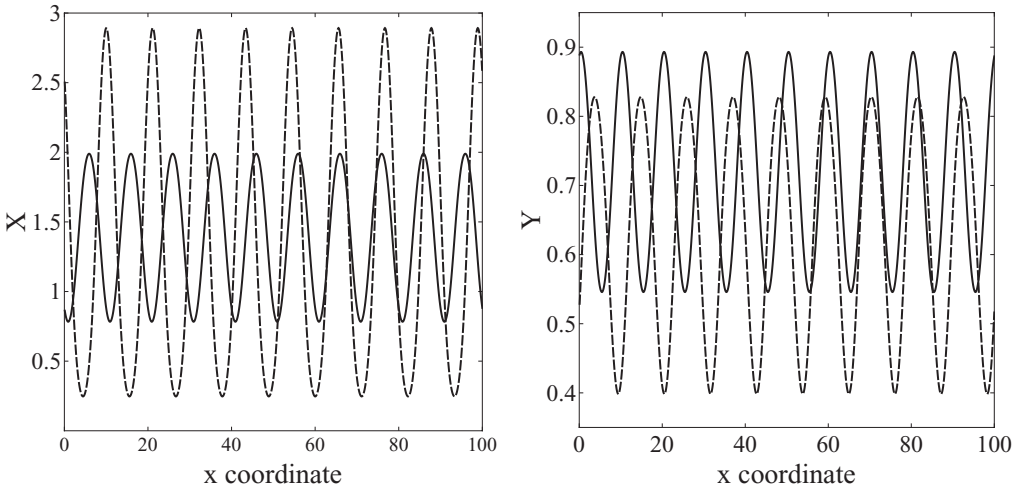

FIG. 4. Concentrations of activator X and inhibitor Y in one layer as a function of position x when $\bar{V} = 0$. The solid lines correspond to $V_r = 50$ and the dotted lines to $V_r = 75$. Patterns are formed due to shear flow alone. Here $\mu = 1.4$ and $R = 25$.

unstable regime. We chose periodic boundary conditions for the variables X_i and Y_i on a one-dimensional spatial domain. We used a finite difference approximation of the spatial derivatives using a grid with points separated by 0.1 dimensionless units of space. The time evolution is carried out using a simple Euler method [17]. The computation runs long enough to reach a steady pattern. We find steady patterns corresponding to higher and lower concentrations of the substances. We first compare two patterns having a flow advecting only the inhibitor with an average velocity equal to zero (Fig. 4). Consequently, patterns will form only in the presence of shear flow. We choose two different relative velocities between the layers where the homogeneous steady state is unstable: $V_r = 50$ and $V_r = 75$. The resulting patterns consist of a series of identical maxima and minima alternating in space. The pattern is stationary in the laboratory frame, which is consistent with the fact that the average flow velocity is zero. The pattern for the larger relative velocity has a larger amplitude (difference between maximum and minimum) as reflected in both substances X and Y. We observe that the pattern with $V_r = 50$ has ten peaks, while the pattern with $V_r = 75$ has nine peaks. This is consistent with the linear stability analysis that predicts a wave number k_m for the maximum growth rate Re λ. This corresponds to a wavelength for fastest growth (defined as $2\pi/k_m$) equal to 10.02 spatial units for $V_r = 50$ and to 11.61 spatial units for $V_r = 75$. These wavelengths can be compared to the distance between peaks in the actual patterns: 10.0 spatial units for $V_r = 50$, and 11.1 spatial units for $V_r = 75$. The real part of the dispersion relation exhibits an interval of unstable wave numbers for $V_r = 50$ [Fig. 1(b)], and for $V_r = 75$. Although some values within this interval have nonzero imaginary parts, the value at the fastest growth rate is a real number. This helps to explain the fact that the patterns in the nonlinear calculations are stationary.

IV. CONCLUSIONS

We have shown that a differential shear flow can lead to pattern formation even when a uniform flow of the same average velocity cannot generate any pattern. Patterns can be generated even if the average flow velocity advecting both substances is zero, as it happens in a system with two layers moving with the same speed but in opposite directions. If this flow advects only the inhibitor, increasing the relative velocity between the layers can make the homogeneous steady state unstable. On the contrary, if the relative velocity advects only the activator, not only does the homogeneous steady state remain stable, but adding shear flow to an already unstable state can stabilize it. The effects of shear flow can be understood by the change of effective diffusivities due to Taylor dispersion. Using this change in the original one-dimensional system provides a very good approximation to the linear stability analysis. The approximation is better if the diffusive coupling between the layers is relatively large. We also carry out numerical solutions of the nonlinear reaction-diffusion-advection equations resulting in spatial patterns in which amplitude, symmetry, and wavelength depend directly on the relative velocity between the layers. The effects of shear flow should be relevant to experiments conducted inside tubes, since viscous boundaries require the velocity to be zero at the walls, thus leading to shear flow. The effects of Taylor dispersion should also apply to other types of flow-induced patterns such as flow-distributed oscillations [2].

ACKNOWLEDGMENTS

This work was supported by the Dirección de Gestión de la Investigación de la Pontificia Universidad Católica del Perú. D.A.V. thanks the Fulbright Commission of Peru for their financial support.

[1] A. B. Rovinsky and M. Menzinger, Phys. Rev. Lett. **69**, 1193 (1992).
[2] P. N. McGraw and M. Menzinger, Phys. Rev. E **68**, 066122 (2003).
[3] M. Kærn and M. Menzinger, J. Phys. Chem. A **106**, 4897 (2002).
[4] A. M. Turing, Philos. Trans. R. Soc. London, Ser. B **327**, 37 (1952).
[5] D. A. Vasquez, Phys. Rev. Lett. **93**, 104501 (2004).
[6] D. A. Vasquez, J. Meyer, and H. Suedhoff, Phys. Rev. E **78**, 036109 (2008).
[7] A. B. Rovinsky and M. Menzinger, Phys. Rev. Lett. **70**, 778 (1993).
[8] R. Tóth, A. Papp, V. Gáspár, J. H. Merkin, D. K. Scott, and A. F. Taylor, Phys. Chem. Chem. Phys. **3**, 957 (2001).
[9] R. A. Satnoianu, J. H. Merkin, and S. K. Scott, Chem. Eng. Sci. **55**, 461 (2000).
[10] R. A. Satnoianu, Phys. Rev. E **68**, 032101 (2003).
[11] P. Gray and S. K. Scott, Chem. Eng. Sci. **39**, 1087 (1984).
[12] R. Satnoianu, J. Merkin, and S. Scott, Phys. Rev. E **57**, 3246 (1998).
[13] R. A. Satnoianu and M. Menzinger, Phys. Rev. E **62**, 113 (2000).
[14] R. A. Satnoianu, P. K. Maini, and M. Menzinger, Physica D **160**, 79 (2001).
[15] G. I. Taylor, Proc. R. Soc. London, Ser. A **253**, 67 (1956).
[16] W. C. Thacker, J. Phys. Oceanogr. **6**, 66 (1976).
[17] S. E. Koonin and D. C. Meredith, *Computational Physics* (Addison-Wesley, Redwood City, CA, 1990).